Surgical Influence on Murine Immunity and Tumor Growth: Relationship of Body Temperature and Hormones with Splenocytes (43377)

HELEN V. RATAJCZAK,*[,1] ROBERT W. LANGE,* ROBERT B. SOTHERN,[†] KAREN L. HAGEN,[‡] PAUL VESCEI,[§] JINYI WU,[‖] FRANZ HALBERG,[‖] AND PETER T. THOMAS*

Department of Life Sciences, IIT Research Institute, Chicago, Illinois 60616; Departments of Surgery[†] and Laboratory Medicine and Pathology,[‖] University of Minnesota, Minneapolis, Minnesota 55455; Research Resources Center,[‡] University of Illinois at Chicago, Chicago, Illinois 60612; and Department of Pharmacology,[§] University of Heidelberg, Heidelberg, Germany

Abstract. **Adrenalectomy predisposed the C3HeB/FeJ Mouse to tumor from a low dose of tumor cells, derived from a C3H spontaneous mammary adenocarcinoma. Sham surgery had a similar effect. In contrast, ovariectomized females, intact females, and male mice did not allow the low dose of cells to develop into a tumor. In order to better understand the role of hormones on the immune system controlling tumor growth, normal C3HeB/FeJ mice were studied for the effect of corticosterone or estradiol on splenic lymphocyte surface antigen expression. Adrenalectomy and ovariectomy caused a decrease in the percentage of all T cell subclasses and an increase in absolute numbers of immunoglobulin-bearing cells. Reconstitution of ovariectomized mice with estradiol did not significantly alter lymphocyte cell surface antigen expression. In contrast, injection of corticosterone into adrenalectomized mice brought these values to normal. Further study on normal mice placed on a 12:12-hr light:dark schedule showed that the hours after lights on (HALO) had a significant effect (analysis of variance) on body temperature, percentage of splenic B cells, T pan, T helper and T suppressor cells, and absolute numbers of T pan cells. Brain dehydroepiandrosterone sulfate correlated positively with T pan lymphocytes, but showed no significant effect on HALO. In contrast, body temperature showed a strong circadian rhythm ($P < 0.001$). In addition, the presentation of estrus was circadian rhythmic ($P = 0.003$) with 58% of mice in estrus at 16 HALO and only 8% at 4 HALO. Multiple regression analysis revealed body temperature was strongly associated with absolute numbers of splenic T lymphocytes and their subsets, as well as percentage of B lymphocytes, Thy 1.2-, and Lyt-2-bearing cells. Similarly, HALO and estrous cycle stage were associated with percentage of T helper cells. The data showed that body temperature and hormones were associated with the cell surface antigens on lymphocytes and suggest that they affect lymphocyte function.** [P.S.E.B.M. 1992, Vol 199]

This laboratory found earlier that the timing within the estrous cycle at which an estrogen receptor-bearing mammary adenocarcinoma was removed by surgical resection afffected the metastatic potential of that tumor in the C3HeB/FeJ mouse (1). If surgery was within a day before ovulation, 40% of the mice were free of metastases as compared with 16% if surgery was carried out on the days following ovulation (1). The data suggested that differences in hormone concentrations were responsible for the different outcomes of surgery in so far as metastases were concerned. These findings have been studied in the human by other investigators. Premenopausal women who underwent breast cancer surgery at about midmenstrual cycle were only one fourth as likely to relapse and die as

[1] To whom correspondence and requests for reprints should be addressed at IIT Research Institute, 10 West 35th Street, Chicago, IL 60616.

Received September 21,1990. [P.S.E.B.M. 1992, Vol 199]
Accepted November 13, 1991.

0037-9727/92/1994-0432$3.00/0

compared with those operated upon during the week preceding or following menstruation (2). In a separate study, overall and recurrence-free survival was greatly reduced in women when the operation was 3–12 days after their last menstrual period (3). These reports dealing with 44 and 249 women, respectively, are seemingly at variance with a study of 81 patients, in which those who underwent surgery near menstruation did not appear to survive longer than those operated on at midcycle (4).

Another group of investigators reported a lack of statistical significance for 245 women in international breast cancer treatment trials (5). Several factors could account for the different findings: The human studies were all retrospective and studied heterogeneous populations. No information was given on the therapy the patients had received. In addition, there was no mention of the time of day (which would reflect different hormone concentrations) at which surgery was performed.

In order to better define the interplay of rhythms in factors that influence the immune response, a study was undertaken in the mouse model using a circadian approach. Because it has been shown that the timing of circadian rhythms in mice was reset by manipulation of the lighting regimen along the 24-hr scale (6), we were able to design an experiment to work at one convenient time. Six boxes were set on six different regimens of onset of light with darkness alternating at 12-hr intervals (12:12-hr light:dark). With a study carried out under such conditions, we have reported a marked circadian rhythm of the percentage and the absolute numbers of the major classes of splenic lymphocytes and of serum corticosterone concentrations in the C3HeB/FeJ mouse (7). The purpose of the present investigation was to expand this work by studying the relationship of body core temperature and hormones to splenic lymphocyte subsets and on the expression of a primary mammary adenocarcinoma in the mouse. Our approach was 4-fold: (i) The effect of hormones on the growth of a primary mammary adenocarcinoma was studied in male and female mice, some untreated, others sham operated, ovariectomized, or adrenalectomized. (ii) The effect of corticosterone and estradiol on splenic cell surface antigen expression was studied in female adrenalectomized and ovariectomized mice, respectively. (iii) The dynamics of body temperature, brain dehydroepiandrosterone sulfate (DHEA-S), serum corticosterone, serum estradiol, and the splenic cell surface antigens were studied, in addition to the circadian presentation of the estrous cycle. (iv) Hormonal, thermal and antigenic associations were analyzed by multiple regression.

Materials and Methods

Mice. Male and female C3HeB/FeJ mice, 3–5 weeks old, were purchased from Jackson Laboratories, Bar Harbor, ME, and quarantined for 2 weeks prior to placement on experiment. Male mice, two per cage, were housed in cages adjacent to those housing females; the latter were housed four per cage. Following surgery, animals were singly housed. All animals had laboratory chow and tap water (saline for adrenalectomized animals) *ad libitum*. Carbon dioxide anesthesia was used prior to exsanguination from the retroorbital plexus. Sera were stored at −70°C prior to hormone analysis.

Surgery. Female mice were adrenalectomized or ovariectomized under anesthesia with Ketamine (75 mg/kg) and Ace Promazine (10 mg/kg). Completeness of ablation was verified by necropsy. The surgical study relating to splenic cell surface antigen expression was carried out in September 1989. The surgical study involving tumor was conducted in June 1990, and observations for tumor growth continued for 4 months.

Tumor. A mammary adenocarcinoma that arose in a female C3H mouse and that was repeatedly carried by subcutaneous transplantation in female C3HeB/FeJ mice was used. Cells were isolated from a tumor approximately 10 mm in diameter, minced with scissors, and suspended in Medium 199 (Gibco Laboratories, Grand Island, NY) supplemented with penicillin (50 units/ml) and streptomycin (50 μg/ml). Cell viability was assessed by trypan blue dye exclusion. Transplantation was accomplished by subcutaneous injection of 2×10^5 viable cells suspended in 0.1 ml of medium into the left hind leg at the base of the tibia.

Circadian Study. This study was conducted during the summer of 1989. Six boxes, 2 × 2 × 2 feet, were constructed of particle board with the advice of Dr. L. E. Scheving. Shielding from outside light was verified by the use of photographic film. For determination of the circadian rhythms and the estrous cycle, 12 females and six males were housed per box. Each box had a timer to set a schedule of light and darkness alternating at 12-hr intervals. Onset of light was staggered by 4 hr between the six boxes. Time is referred to as hours after lights on (HALO). One half of the females were sacrificed by exsanguination on Day 27 and the remainder on Day 28. Three of the boxes were placed in each of two rooms with opposite 12:12-hr light:dark cycles. The boxes were thus opened either in light or darkness at one time, with the HALO simulating a 24-hr day. Cages were cleaned once a week on the same day of the week.

Estrous Cycle. After standardization for at least 2 weeks in the boxes, a vaginal smear of each female mouse was taken daily, followed by the rectal temperature. Smears were fixed in absolute methanol and stained with hematoxylin and eosin. Relative numbers of cornified, nucleated epithelial, and polymorphonuclear cells were scored 0 to 3+. Stage of the cycle was assigned to published criteria (8, 9).

Lymphocyte Surface Antigen Determination. Spleens were aseptically removed and single cell sus-

pensions were prepared in (No. 330–1420; Gibco) (pH 7.6) plus 0.1% NaN_3. Lymphocyte cell surface antigens were identified using an Epics V flow cytometer equipped with a 488-nm argon laser (Coulter Electronics, Hialeah, FL). Cells were stained with antibodies conjugated with fluorescein isothiocyanate; monoclonal antibodies to Thy 1.2 (T pan), L3T4 (T helper), and Lyt 2 (T suppressor) were purchased from Becton Dickenson, Mountain View, CA. F(ab′)2 goat antimouse immunoglobulins (Zymed, South San Francisco, CA) were used to identify B cells. Exclusion of propidium iodide (Sigma, St. Louis, MO) determined cell viability; only viable cells were analyzed.

Hormones. Radioimmunoassay was used to quantify serum concentrations of corticosterone and estradiol (Radioassay Laboratory, ICN Biomedical, Inc., Plainview, NY) and DHEA-S in the brains (Pharmakologisches Institut der Universitat Heidelberg, Heidelberg, Germany). Adrenalectomized or ovariectomized mice were given corticosterone (100 μg/injection Sigma) or estradiol (5 μg/injection; Sigma) or vehicle (sesame oil; Sigma) by subcutaneous injection 24 and 48 hr prior to identification of splenic cell surface antigens.

Statistics. The least squares fit of a 24-hr cosine curve with the precaution of the cosinor method (10) was used to assess rhythmicity of cell surface antigen expression and hormone concentrations. Multiple regression analysis, chi-square, and Pearson product-moment correlations were also used. Where appropriate, data were transformed to logarithms, logits, or cosines prior to analysis. Analysis of variance was followed by post hoc comparisons of groups using Student's t test.

Results

Effect of Hormonal Ablation on Tumor Growth. The influence of corticosterone and estradiol on the ability of a primary mammary adenocarcinoma to grow was studied in several groups indicated in Figure 1. Each group was divided into two subgroups: one received 2×10^5 and the other 2×10^3 viable tumor cells. Mice were observed for tumor growth for 4 months. Some animals of each group did not develop palpable tumors. All groups that received the high dose had tumor incidence (60–89%). Intact animals that received the low dose of tumor cells did not develop tumors, nor did ovariectomized females. In sharp contrast, adrenalectomized or sham-operated females developed tumors whether the dose was high or low.

Effect of Corticosterone and Estradiol on Splenic Lymphocyte Subsets. Corticosterone and estradiol versus splenic lymphocyte subsets were studied in female mice not inoculated with tumor (Fig. 2). The animals were surgically altered by adrenalectomy or ovariectomy. The effect of surgery was reflected in lowered concentrations of the respective hormones. The groups were divided into two; one group received injections of corticosterone or estradiol, while the other received oil only. Splenic cell surface antigens were identified by flow cytometry; the whole population of T cells was identified by fluorescein isothiocyanate-conjugated antisera to Thy 1.2, T helper cells by anti-L3T4, and T cytotoxic cells by anti-Lyt2. B lymphocytes were identified by antisera to immunoglobulin. Serum concentrations of estradiol and corticosterone were measured by radioimmunoassay. The percentage of splenic cell surface antigens for each of the T cell antigens was lowered in contrast to B cells, which were unaffected. The percentage of T cell antigens in splenocytes from ovariectomized mice injected with estradiol were not restored to that of normal mice. Adrenalectomized mice given corticosterone had elevated percentages of each, with Thy 1.2 being brought to normal levels. The absolute numbers presented a different picture (data not shown). Numbers of Ig-bearing lymphocytes increased in surgically altered mice, with no increase of any of the T antigens. Again, estradiol injection in ovariectomized animals did not affect the numbers significantly. However, injection of corticosterone in adrenalectomized animals brought numbers of B lymphocytes to normal levels.

Body Temperature, Concentration of Brain DHEA-S, Serum Corticosterone, Serum Estradiol, and Splenic Cell Surface Antigen Expression. Twelve mice were placed in each of six boxes with the lights on for 12:24 hr, with light onset staggered between boxes by 4 hr. Mice were anesthetized with carbon dioxide and exsanguinated. Their spleens and brains were removed. Splenic cell surface antigen expression was measured by flow cytometry. Brains were immediately frozen in liquid nitrogen, and subsequently homogenized in acetone and evaporated to dryness prior to radioimmunoassay for DHEA-S. The data for body temperature, hormones, and splenic cell surface antigen expression were mapped (Figs. 3 and 4). The circadian aspects of corticosterone and cell surface antigens have been reported previously (7). When the body temperatures of the 72 animals were tested for a circadian rhythm by the least squares fit of a 24-hr cosine curve, a strong circadian rhythm was revealed ($P < 0.001$). In contrast, the assumption of no circadian rhythm could not be rejected for concentration of DHEA-S in the brains. Analysis of variance for differences among the means at each HALO time revealed significant differences for body temperature, percentage of each cell subset, and absolute numbers of Thy 1.2-bearing cells. Concentration of brain DHEA-S was found to be positively correlated with absolute numbers of Thy 1.2-bearing cells ($P < 0.05$).

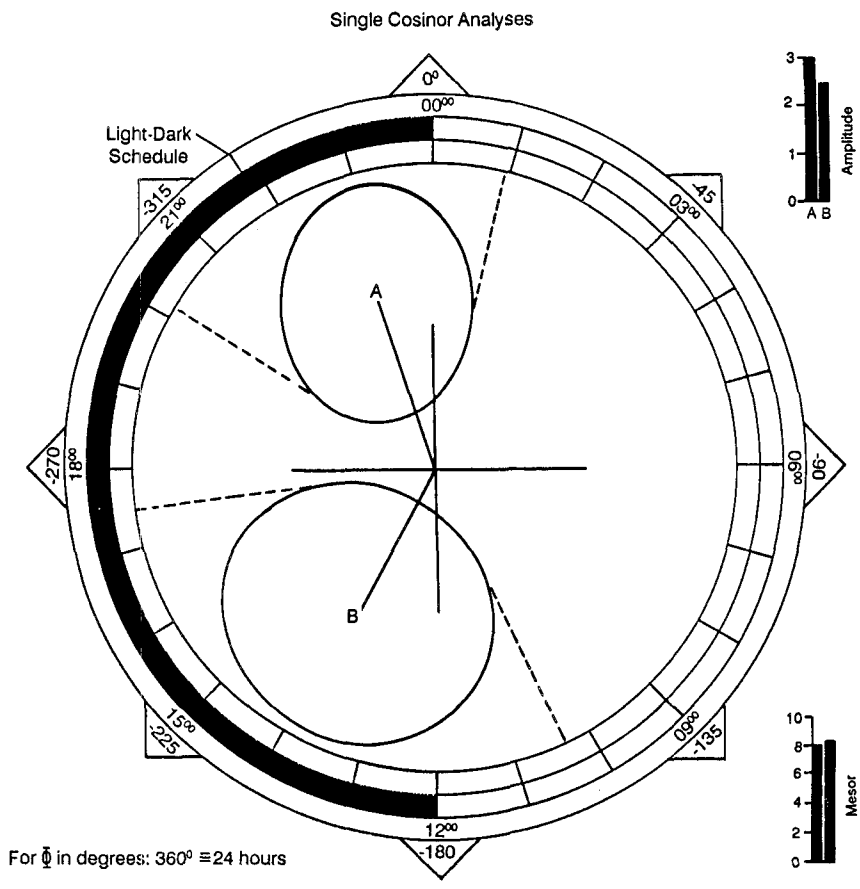

Key	P	N	PR	Mesor +- SE	Amplitude*	Acrophase (Φ) •
A Proestrus	0.005	12	70	8.06 0.45	2.98(1.06 4.92)	-342°(-302 -14)
B Metestrus	0.011	25	34	8.26 0.54	2.45(0.53 4.)	-209°(-155 -263)

P = Probability of Hypothesis: Amplitude=0; N=Number of Observations
PR = Percent Rhythm (percentage of variability accounted for by cosine curve)
• Conservative 95% confidence limits (parentheses) derived from cosinor ellipse

Figure 1. Effect of hormones on growth of a primary mammary adenocarcinoma. Mice were adrenalectomized or ovariectomized. Immediately after surgery, the animals were injected with 2,000 (Lo dose) or 200,000 (Hi dose) viable tumor cells in the left hind leg at the ankle and observed for tumor development for 4 months. • *P*-value, chi-square.

Estrous Cycle Stage Incidence as a Function of HALO Time. In order to determine that the mice were undergoing regular estrous cycling, the body temperature and vaginal smear from each mouse were recorded daily for 17 days prior to sacrifice. The series of vaginal smears was also used to determine the phase of the estrous cycle at the time of the lymphocyte study. Presentation of estrus was found to be circadian rhythmic (Table I). Fifty-eight percent of the animals were in estrus when tested at 16 HALO (early dark/activity span), while only one out of the 12 mice (8.3%) was in estrus at 4 HALO (early light/sleep span) (rhythm detection significant at $P < 0.003$ from fit of 24-hr cosine). Similarly, more mice were in metestrus or diestrus when sampled in the light span as compared with the dark span (rhythm detection significant at $P = 0.010$ from fit of 24-hr cosine). Large circadian variations and the unequal distribution of animals in each estrus stage at each circadian stage undoubtedly obscured any effect of estrous stage in the analyses.

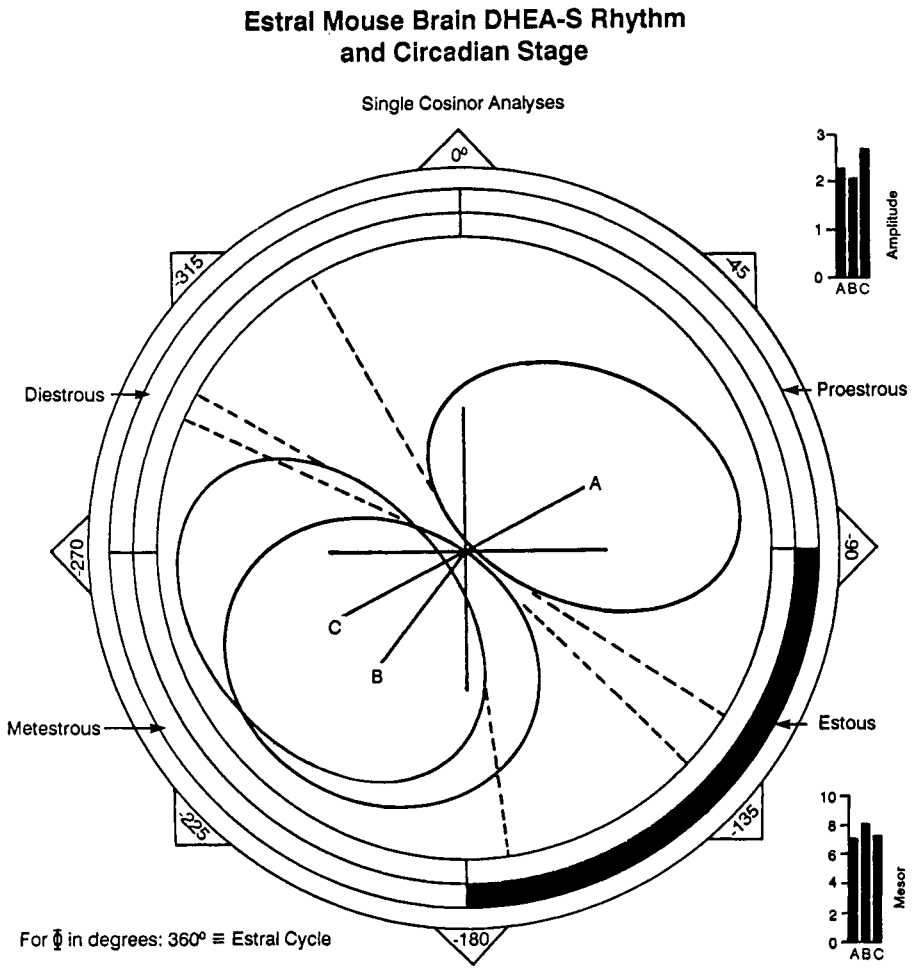

Key	P	N	PR	Mesor +- SE	Amplitude*	Acrophase (Φ) *
A 0400 Halo	0.085	12	42	7.02 0.71	2.29(0.10 4.71)	-62° (-332 -124)
B 0800 Halo	0.099	11	45	8.05 0.65	2.06(0.04 4.09)	-218°(-135 -296)
C1200 Halo	0.045	12	50	7.32 0.76	2.68(0.48 5.00)	-242°(-173 -301)

P = Probability of Hypothesis: Amplitude=0; N=Number of Observations
PR = Percent Rhythm (percentage of variability accounted for by cosine curve)
* Conservative 95% confidence limits (parentheses) derived from cosinor ellipse

Figure 2. Percentage of splenic cell surface antigens in surgically altered mice. Mice were ovariectomized (OX) or adrenalectomized (AX). One week later, groups were injected subcutaneously with oil or hormone 24 hr and 48 hr prior to identification of splenic cell surface antigens (10 mice/group). Two animals per group were injected only at −24 hr. Statistics:

Group	Thy 1.2	L3T4	Lyt2	IgG
Normal vs OX + Oil	0.012*	0.001	0.005	NS
OX + E2	0.004	0.0001	0.001	0.029
AX + Oil	0.001	0.001	0.0001	NS
AX + Cort	NS	0.001	0.004	NS
OX + Oil vs OX + E2	NS	NS	NS	NS
AX + Oil	NS	NS	NS	NS
AX + Cort	NS	NS	NS	NS
OX + E2 vs AX + Oil	NS	NS	0.022	NS
AX + Cort	NS	NS	NS	NS
AX + Oil vs AX + Cort	0.038	NS	0.012	NS

* *P*-values, Student's *t* test. Abbreviations: E2, estradiol, 5 μg/mouse; cort, corticosterone, 100μg/mouse.

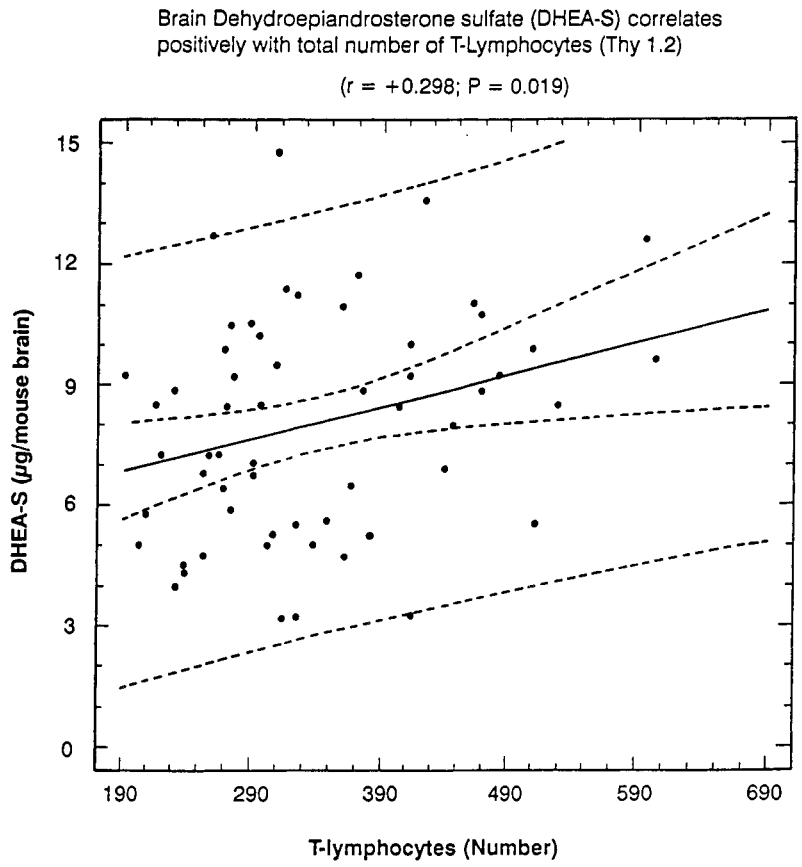

Figure 3. Chronograms of body temperature, brain DHEA-S, serum corticosterone, and serum estradiol. Twelve animals were measured at each HALO. Mice were anesthetized with carbon dioxide and exsanguinated from the retroorbital plexus, and their brains were removed. The sera and brains were frozen and hormones were subsequently measured by radioimmunoassay. The bars represent SE.

Relative Influence of Body Temperature and Hormones on Lymphocyte Subsets. Multiple regression served to analyze the data set for the relative association of fluctuations in body temperature, serum corticosterone, serum estradiol, brain DHEA-S, HALO, and estrous cycle stage with the expression of cell surface antigens. Body temperature was outstanding in association with the percentage of Thy 1.2, Lyt2, and Ig-bearing cells, with HALO and estrous cycle stage also associated with percentage of L3T4-bearing cells. Body temperature was associated with absolute numbers of Thy 1.2, Lyt2, and L3T4. Significance levels ranged from 0.00005 to 0.002.

Discussion

The body temperature association with the percentage and absolute numbers of splenic lymphocyte subsets is noteworthy. An intimate association of body temperature and the immune response has long attracted attention. Since the first quarter of this century, it has been known that fever can help cure certain diseases. Indeed, Dr. Julius Wagner-Jauregg won the Nobel Prize for Physiology and Medicine in 1927 for his treatment of dementia paralytica with malaria vaccine. Perhaps some beneficial effect of fever lies in its modulation of the immune response in addition to any direct effect of killing microorganisms. In the current study, the temperature fluctuation was only that within the circadian and estrous cycles of normal mice, and clearly did not include a fever. Nonetheless, very strong correlations were found with every cell subset studied.

It has been reported that in the human the T helper to T suppressor cell ratio undergoes a rhythm similar to that of the menstrual cycle (11). The current study did not support that result. No correlation between percentage or absolute number of lymphocyte subsets occurred with phases of the estrous cycle. However, the interplay of the hormones with the estrous cycle and cell surface antigen expression was suggested. In addition, there were other findings similar to those in the human: The body temperature increased after ovulation (data not shown), similar to the pattern of body temperature in the human during the menstrual cycle (12). Also, the body temperature was increased during the active phase (dark span), similar to the human, in whom the body temperature is higher during the active phase (usually the light span).

In the present circadian study, not only did temperature explain a significant proportion of lymphocyte subsets, both percentages and absolute numbers, but

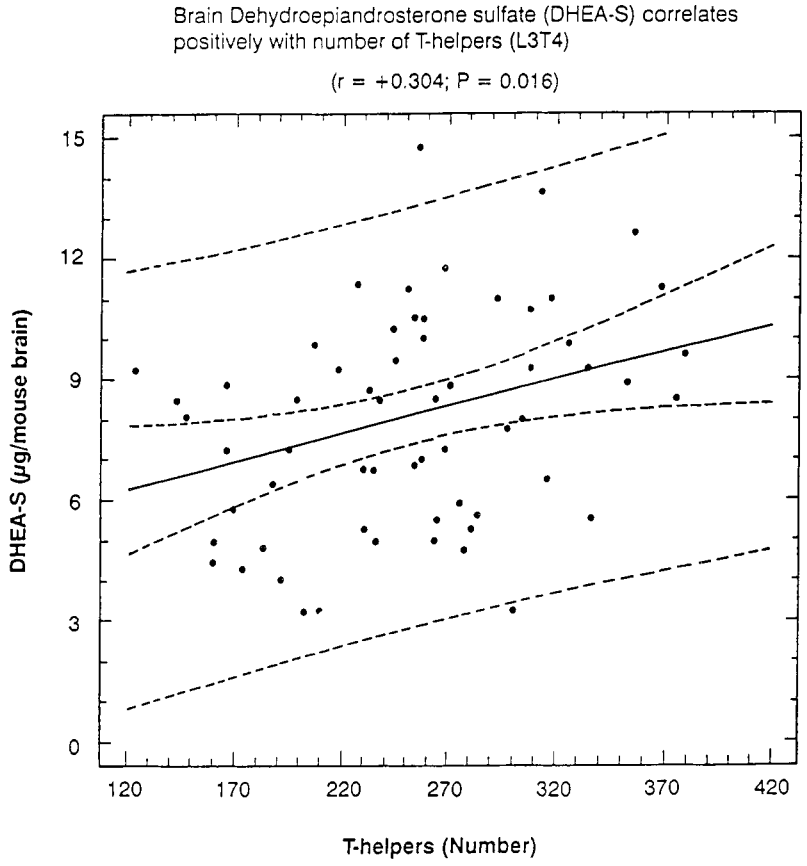

Figure 4. Chronograms of percentages and absolute numbers of splenic lymphocyte subsets: B cells, T pan, T helper, and T suppressor cells. Following the removal of the brain, the spleen of each animal was aseptically removed, brought to a single cell suspension, and stained for lymphocyte subsets using fluorescein isothiocyanate-conjugated antisera specific for each subset. Subsets were determined by flow cytometry.

Table I. Estrous Stage Incidence vs Circadian Stage for C3HeB/FeJ Female Mice

Estrous stage	Time (hr after lights on in LD 12:12)[a]							
	Total (*n*)	00 (*n*) (%)	04 (*n*) (%)	08 (*n*) (%)	12 (*n*) (%)	16 (*n*) (%)	20 (*n*) (%)	Time-effect *P*[b]
Proestrus	12	1 (8.33)	4 (33.33)	4 (33.33)	2 (16.67)	0 (0.00)	1 (8.33)	0.041
Estrus	25	3 (25.00)	1 (8.33)	3 (25.00)	6 (50.00)	7 (58.33)	5 (41.67)	0.003
Metestrus	25	5 (41.67)	6 (50.00)	3 (25.00)	4 (33.33)	3 (25.00)	4 (33.33)	0.267
Diestrus	10	3 (25.00)	1 (8.33)	2 (16.67)	0 (0.00)	2 (16.67)	2 (16.67)	0.422
Proestrus and estrus	37	4 (33.33)	5 (41.67)	7 (58.33)	8 (66.67)	7 (58.33)	6 (50.00)	0.010
Metestrus and diestrus	35	8 (66.67)	7 (58.33)	5 (41.67)	4 (33.33)	5 (41.67)	6 (50.00)	0.010

[a] Twelve mice per timepoint (total = 72).
[b] *P*-value derived from zero-amplitude test by least squares fit of a 24-hr cosine.

HALO and estrous cycle stage also contributed, affecting percentage of T helper cells. The corticosterone concentrations were higher than expected, probably due to the stress imposed by the method of anesthetization and bleeding (from the retroorbital plexus). In future experiments, greater care should be taken to ameliorate stress when studying stress-related hormones.

It should be noted that it is unclear whether the statistically associated parameters are causally linked. It is entirely possible that they were simply parallel outcomes of multiple regulatory phenomena influenced similarly by circadian rhythms. To address this issue, the surgical experiments were performed. They showed that ovariectomy and adrenalectomy have an effect on immunity. Ovariectomy and adrenalectomy lowered percentages of splenic T lymphocyte subsets and increased absolute numbers of B lymphocytes. The difference in pattern of expression between percentages

and absolute numbers of lymphocytes may relate to the changing numbers of cells in the spleen due to the recirculation of lymphocytes. The total number of splenocytes was not constant at each HALO. But, unlike the percentages of subsets, the total number did not display a circadian rhythm. Therefore, lymphocytes without T or B cell antigens must also fluctuate. Other lymphocyte subsets in addition to T and B cells should be studied in the model, particularly natural killer cells that would be heavily involved in prevention of a low dose of tumor cells from growing in a naive animal.

Another effector is DHEA-S, which has a negative correlation with risk of developing breast cancer (13). In the present study, DHEA-S in the brain correlated positively with absolute numbers of T pan cells, supporting the association of low levels of DHEA-S with risk of developing breast cancer, using the logic that the T cells help to prevent the tumor from growing. The data also support the recent finding that dietary DHEA inhibited rat mammary gland chemical carcinogenesis (14).

Treatment of ovariectomized animals with estradiol did not statistically influence the percentage or absolute number of the T lymphocyte subsets in contrast to treatment of adrenalectomized mice with corticosterone. The latter animals had percentages of T lymphocyte subsets that were comparable to those of intact animals. In addition, these animals had similar absolute numbers of B cells. Surgery itself may have elevated corticosterone in the ovariectomized animals. The effects of corticosterone on cell surface antigens were prominent, and imply that corticosterone is intimately involved with the immune response, since cell surface antigens reflect cell function (15).

In addition, the present experiment involving surgically altered mice in which high and low numbers of mammary adenocarcinoma cells were injected supports the role of corticosterone and estradiol in the immune response. The mice were injected with tumor immediately following surgery. All groups of mice inoculated with the high dose of tumor cells developed tumor. In contrast, there was a marked difference among the groups receiving the small dose of cells. For intact and ovariectomized females and intact male mice, the smaller inoculum of mammary adenocarcinoma cells failed to develop into a tumor. In adrenalectomized animals and sham-operated females, the tumor developed from the low as well as the high dose. In surgically stressed animals with normal or low corticosterone, immunosuppression occurred and the low dose of tumor cells grew, in contrast to surgically stressed animals with low estradiol, in which the immune response was intact and the tumor did not grow. What matters may well be the timing and relative concentrations of the hormones, rather than merely the dose of tumor cells. Hormones were thus shown to affect nonspecific mechanisms of prevention of tumor growth, because the mice had not been exposed to the tumor before. In the prior study (1), hormones were shown to affect metastasis subsequent to surgical removal of the tumor. In that study, specific cytotoxicity was probably involved because the mice had had the tumor for a sufficient period of time for sensitization to occur.

These data clearly show the interplay of body temperature, hormone concentration, and immunity, as shown by lymphocyte surface antigen expression and the ability to reject low doses of tumor. The parameter with the strongest correlation with cell surface antigen expression was body temperature, a finding that invites greater scrutiny. In the case of corticosterone, a casual association was proved with respect to expression of Thy 1.2. For the other associations, one must use caution in extending an association to imply that a change in one caused a change in the other.

These findings should be helpful in designing prospective studies in the human to help define the best milieu for surgical intervention in attempts to cure breast cancer. Further work will be required to extend the findings to other types of tumors or to manipulation of the immune system.

This work was supported by Grant 1161 from IIT Research Institute and U.S. Public Health Service Grants GM 13981 and HLB 40650.

1. Ratajczak HV, Sothern RB, Hrushesky WJM. Estrous influence on surgical cure of a mouse breast cancer. J Exp Med **168**:73–83, 1988.
2. Hrushesky WJM, Bluming AZ, Gruber SA, Sothern RB. Menstrual influence on surgical cure of breast cancer. Lancet **2**:949–952, 1989.
3. Badwe RA, Gregory WM, Caudary MA, Richards MA, Bentley AE, Rubens RD, Fentiman IS. Timing of surgery during menstrual cycle and survival of premenopausal women with operable breast cancer. Lancet **337**:1261–1264, 1991.
4. Powles TJ, Jones AL, Ashley S, Tidy A. Menstrual effect on surgical cure of breast cancer [Letter]. Lancet **2**:1343–1344, 1989.
5. Gelber RD, Goldhirsch A. Menstrual effect on surgical cure of breast cancer [Letter]. Lancet **2**:1344, 1989.
6. Halberg F, Barnum CP, Silber RH, Bittner JJ. 24-Hour rhythms at several levels of integration in mice on different lighting regimens. Proc Soc Exp Biol Med **97**:897–900, 1958.
7. Lange R, Ratajczak H, Thomas P, Hagen K, Wu J, Halberg F. Circadian rhythms in expression of cell surface antigens of murine spleen cells. In: Reinberg A, Smolensky M, Labrecque G, Eds. Annual Review of Chronopharmacology Oxford: Pergamon Press, Vol **7**: pp223–226, 1990.
8. Bronson FH, Dagg CP, Snell GD. Reproduction. In: Green EL, Ed. Biology of the Laboratory Mouse. New York: McGraw-Hill Book Co., pp187–204, 1966.
9. Barkley MS, Bradford GE. Estrous cycle dynamics in different strains of mice. Proc Soc Exp Biol Med **167**:70–77, 1981.
10. Nelson W, Tong YL, Lee JK, Halberg F. Methods for cosinor-rhythmometry. Chronobiologia **6**:305–323, 1979.
11. Krzanowski M. Low human T4:T8 lymphocyte ratios around ovulation time. Chronobiologia **12**:254, 1985.

12. Simpson HW, Halberg EE. Menstrual changes of the circadian temperature rhythm in women. In: Ferin M, Halberg F, Richart RM, Van de Wiele RL, Eds. Biorhythms and Human Reproduction. New York: John Wiley and Sons, pp549–556, 1974.
13. Halberg F, Cornelissen G, Sothern RB, et al. International geographic studies of oncological interest on chronobiological variables. In: Kaiser H, Ed. Neoplasms: Comparative Pathology of Growth in Animals, Plants, and Man. Baltimore: Williams and Wilkins, pp553–596, 1981.
14. Ratko TA, Detrisac CJ, Mehta RG, Kelloff GJ, Moon RC. Inhibition of rat mammary gland chemical carcinogenesis by dietary dehydroepiandrosterone or a fluorinated analogue of dehydroepiandrosterone. Cancer Res **51**:481–486, 1991.
15. Walker KD, Hogarth PM, Murray PJ, Lovering KE, Classon BJ, Chambers GW, McKenzie IFC. Ly antigens associated with T cell recognition and effector function. Immunol Rev **82**:47–77, 1984.

Does Aging Affect Liver Microtubules? (43378)

LAVENTRICE TAYLOR,*,† ALBERT L. JONES,*,†,‡,§ AND DOUGLAS L. SCHMUCKER*,†,§,[1]

Cell Biology and Aging Section, Department of Veterans Affairs Medical Center, San Francisco, California 94121; Departments of Anatomy† and Medicine‡ and the Liver Center,§ University of California, San Francisco, California 94143*

Abstract. **Microtubules are essential for many cell processes, e.g., ligand-receptor endocytosis and the vectorial movement of endosomes. The cytoskeleton, particularly microtubules, may undergo age-related changes that are reflected in cell dysfunctions. For example, the translocation of ^{125}I-IgA-containing vesicles from the sinusoidal surface to the pericanalicular cytoplasm is reduced (>40%) in old versus young rats. Electron microscopic analysis demonstrated that the concentration of microtubule profiles in young animals is within 10–20% of that in old rats. The relative concentration of polymerized tubulin declines >70% by 12 months of age, but the total tubulin content remains unchanged until later, i.e., declining 50% by 24 months. Concomitant increases occur in the free fractions of microtubule-associated proteins (MAP), i.e., MAP$_1$ and heat-stable MAPS. These fractions are not associated with polymerized tubulin. The declines in total and polymerized tubulin, together with the increases in the MAPS' free fractions, may be indicative of fewer and/or shorter microtubules. These data lend credence to the supposition that aging is accompanied by perturbations of microtubule functions that ultimately are expressed as biomarkers characteristic of aging.**

[P.S.E.B.M. 1992, Vol 199]

Cytoplasmic microtubules are essential for a variety of cellular processes, including ligand-receptor endocytosis and the subsequent vectorial movement of ligand-containing vesicles destined for secretion or degradation (see Ref. 1 for a review). The maintenance of these functions depends on a stable polymer to monomer tubulin ratio, an autoregulated process (2–4). Caron *et al.* (5) have shown that the autoregulation of tubulin synthesis and the processing of endocytosed ligands are sensitive to small changes in this critical ratio. Since tubulin constitutes approximately 1% of the total hepatic protein composition and aging is accompanied by shifts in the synthesis and intracellular concentrations of numerous hepatic proteins, age-associated changes in the rate of tubulin synthesis or in the tubulin polymer to monomer ratio may contribute to concomitant alterations in microtubule-dependent functions (6; see Ref. 7 for a review).

There is some evidence that the cytoskeletal system, particularly microtubules, undergoes age-related changes that are reflected in cellular dysfunctions (8). In rat hepatocytes, for example, the transport of IgA and anticholera toxin IgA antibodies from the blood to the bile declines up to 6-fold between 3 and 25 months of age (9, 10). The hepatocellular translocation of vesicles containing endocytosed IgA and another glycoprotein, horseradish peroxidase, is significantly impaired, 60% and 40%, respectively, in rats pretreated with the microtubule depolymerizing agent, colchicine (3, 4). A similar decline (>40%) in the translocation of IgA-laden vesicles occurs in untreated rat hepatocytes as a function of aging alone (9). Microtubule integrity may be essential for the transport of newly synthesized IgA receptor (secretory component), a nonrecycled glycoprotein, to the hepatocyte plasma membrane (4). Interestingly, a 4-fold loss of IgA receptors from hepatocyte plasma membranes accompanies aging in the rat (11). Since endocytosed IgA does not get transported to the bile canaliculus in old rats, the number of IgA receptors is diminished in these animals, and colchicine elicits a similar decline in the hepatobiliary transport of IgA in young rats, we speculated that aging may be accompanied by microtubule dysfunction, e.g., reduced tubulin synthesis, altered tubulin polymer to monomer ratio that culminates in impaired cell function(s). Since microtubule associated proteins (MAPS) are essential to optimal microtubule function, changes in the quality

[1] To whom requests for reprints should be addressed at Cell Biology and Aging Section (151E), Department of Veterans Affairs Medical Center, 4150 Clement Street, San Francisco, CA 94121.

Received May 20, 1991. [P.S.E.B.M. 1992, Vol 199]
Accepted November 13, 1991.

0037-9727/92/1994-0441$3.00/0

or quantity of these components may also contribute to an age-related dissociation of the cytoskeleton. The present study describes results from a correlated structural and biochemical analysis of rat hepatocyte microtubules as a function of aging.

Methods

Animals. Male Fischer 344 (CDF) rats, aged 3–6 months (young), 12–16 months (mature), and 24–30 months (old; <50% survivorship), obtained from the National Institute on Aging colony (Harlan Industries, Inc., Indianapolis, IN), were used throughout the study. The animals were maintained under barrier conditions and fed laboratory chow and water *ad libitum* in accordance with the guidelines of the Committee on Care and Use of Laboratory Animals of the Institute of Laboratory Animal Resources. All of the rats were subjected to a 12-hr fast prior to sacrifice to minimize the hepatic content of glycogen, which interferes with morphologic and biochemical analyses.

Electron Microscopic Analysis. Six young and six old animals were anesthetized with sodium pentobarbital, their livers were perfused via the hepatic portal vein with 2.7% glutaraldehyde and 0.8% paraformaldehyde in 0.2 *M* sodium bicarbonate, buffer, and the tissue was prepared for electron microscopic examination (12). Six tissue blocks, three from Zone 1 and three from Zone 3, were selected from each of the animals, and five electron micrographs per tissue block were taken and enlarged to a final magnification of ×45,000. The photographic fields were chosen according to an unbiased, systematic sampling procedure which required that the grid squares be covered with hepatocyte cytoplasm, two sides of the field be defined by grid bars, and the field be devoid of nuclear profiles. This sampling yielded 180 micrographs/age group and a total of 360 fields for analysis. Each micrograph was reviewed and every identifiable microtubule profile, regardless of length, was scored, as was each peroxisome in the same field. Peroxisomes were selected as the internal standard, since previous quantitative analysis demonstrated that the relative volume of this organelle compartment remains unchanged during aging in Fischer 344 rats (12). The data were expressed as the number of microtubule and peroxisome profiles per unit area of hepatocyte cytoplasm (five photographic fields) and as the ratio of microtubule to peroxisome profiles.

Quantitative Analysis of Tubulin and MAPS. Total and free tubulin as well as MAPS concentrations were determined in high-speed supernatants prepared from liver as described previously (13). Livers were homogenized in 2 vol (w/v) of Mes buffer (100 m*M* 2-[*N*-morpholino]ethanesulfonic acid, 0.5 m*M* $MgCl_2$, and 1.0 m*M* EGTA) with or without 4 *M* glycerol. Homogenates were centrifuged for 60 min at 100,000 *g* and the resultant supernatants were used to measure free (with glycerol) and total (without glycerol) tubulin.

Mouse monoclonal anti-α-tubulin and mouse monoclonal anti-β-tubulin antibodies of known specificities (Amersham) were used to quantitate α- and β-tubulin, respectively (14). MAP_1 content of the supernatants was measured using a monoclonal anti-MAP_1 antibody (clone HM-1; Sigma), which reacts with MAP_1 only. MAP_2 and tau were measured with a polyclonal rabbit anti-MAPS antibody (Sigma), which reacts only with these heat-stable MAPS. Biotinylated goat antimouse IgG and biotinylated goat antirabbit IgG were supplied by Cappel. The specificities of the antibodies were assessed by Western blot analysis (data not shown).

The relative amounts of α- and β-tubulin, MAP_1, MAP_2, and tau were determined by enzyme-linked immunosorbent assay. Microtiter plates were coated with serially diluted liver supernatants. Plates were incubated with a 1/1000 dilution of anti-α-tubulin, anti-β-tubulin, anti-MAP_1, or anti-MAPS mouse antibody. Wells were reacted with biotinylated goat antimouse IgG or biotinylated goat antirabbit IgG, avidin-conjugated horseradish peroxidase (Vector), and *ortho*-phenylenediamine (Zymed). The reaction product was stopped with 2 *N* sulfuric acid and the absorbance was measured at 490 nm. Since tubulin is a highly conserved protein, bovine brain tubulin purified according to the method of Sloboda *et al.* (15) was used as a tubulin standard. Standard curves were established for α- and β-tubulin using the corresponding monoclonal antibody. Liver tubulin values were calculated from the linear portion of the standard curves and are the result of the addition of α- and β-tubulin concentrations.

Results

A reassessment of stereologic and quantitative autoradiographic data generated in a previous study demonstrated that the translocation of ^{125}I-IgA-containing endocytic vesicles from the hepatocyte sinusoidal surface to the bile canaliculus is reduced by at least 40% in old versus young rats (9). This reduction reflects differences in vesicle movement or number rather than in ^{125}I-IgA autoradiographic grain density, since vesicles in young and old rats contained 29% and 26%, respectively, of the total grains counted in the hepatocytes.

Neither the morphologic appearance nor the relative concentration of hepatocyte microtubule profiles, i.e., the number per uniform area of hepatocyte cytoplasm, changed appreciably between 6 and 30 months of age (Table I). The microtubule profile densities estimated in young and old rats were within 10% of each other. The number of peroxisomes in the same photographic fields was similar in both age groups, i.e., within 15%. Furthermore, expression of the microtubule pro-

Table I. Effect of Aging on the Number of Rat Hepatocyte Microtubule and Peroxisome Profiles[a]

Age (mos)	Microtubules (no./unit area)[b]	Peroxisomes (no./unit area)	Microtubules/ peroxisomes
6	2.8 ± 1.9	13.3 ± 2.7	0.21
30	3.1 ± 1.8	11.1 ± 3.4	0.28

[a] Values represent the means of six rats (180 photographic fields) ± SD.
[b] Data expressed as the number of organelle profiles per unit area of hepatocyte cytoplasm; a unit area constitutes the cytoplasmic area included within five photographic fields at a final magnification of ×45,000.

files relative to the number of peroxisomes yielded similar ratios in young and old animals, 0.21 and 0.28, respectively.

On the other hand, biochemical analysis revealed several age-related changes in the concentrations of liver tubulin and MAPS (Table II). Increasing age is accompanied by a shift in the free to total (α and β) tubulin ratio, i.e., a 2-fold increase in mature and old animals in comparison to young rats. The free tubulin fraction constitutes 45% of the total tubulin pool in young rats, but this fraction increases to 85% and 88% in mature and old animals, respectively. This shift is not due to a unilateral increase in the free tubulin fraction, but appears to be a consequence of an increase in the free tubulin content in mature rats and a decline in the total tubulin content of old animals. The hepatic content of polymerized α- and β-tubulin exhibits a decline from 2.6 to 0.7 to 0.3 mg/g liver in 3-, 12-, and 24-month-old rats, respectively. While a concomitant change in the total MAP_1 concentration appears to be inconsequential, there is a >3-fold increase in the free fraction (Table II). A more pronounced shift occurs in the heat-stable MAPS, i.e., MAP_2 and tau. The concentration of total heat-stable MAPS declines >40%, whereas the corresponding free fraction(s) increases nearly 2-fold with increasing age.

Discussion

Circumstantial evidence from several laboratories, including our own, suggests that microtubule dysfunction accompanies aging (16; see Ref. 8 for a review). Quantitative electron microscopic autoradiographic data from a previous study suggested that the microtubule-dependent movement of IgA-containing vesicles from the sinusoidal surface of hepatocytes to the bile canalicular membrane was impaired in rats with increasing age (9). The distribution of radiolabeled IgA to endocytic vesicles was similar in young and old rats, thus eliminating differences in grain density as a possible explanation. While we cannot exclude the possibility of an age-related shift in the number of endocytic vesicles, the nonpericanalicular cytoplasmic compartments in both age groups contained equal numbers of autoradiographic grains, suggesting that the endosome population is reasonably stable during aging. An alternative explanation is that the nonpericanalicular vesicle pool is saturated in young and old animals and, thus, the difference in the pericanalicular cytoplasm is a reflection of reduced translocation alone.

On the basis of these data, a correlated structural and biochemical analysis appeared to be a logical approach to the question of whether or not aging compromises hepatic microtubules. The mean number of microtubule profiles per unit area of hepatocyte cytoplasm was reasonably consistent, regardless of animal age. Since the volume density of the peroxisome compartment is unaffected by aging in the Fischer rat, it provides an excellent internal standard to compare shifts in the density of other organelles, e.g., microtubules (12). The absence of a significant shift in the hepatocyte microtubule to peroxisome profile ratio suggests that if aging affects microtubule function, correlated morphologic changes are more subtle. This probably reflects the low frequency of microtubule profiles observed in both age groups and the relatively small sample of liver tissue examined.

The age-related decline in total tubulin concentrations, as well as the increase in the free to total tubulin ratio, may be indicative of fewer intact microtubules. A shift in the latter parameter may go undetected in a morphologic analysis, since microtubule length cannot

Table II. Effect of Aging on the Concentrations of Rat Liver Tubulin (α and β) and Microtubule-Associated Proteins (MAP_1 and Heat-Stable MAPS)[a]

Age (mos)	Tubulin[b]		MAP_1[c]		Heat-stable MAPS[c]	
	Total	Free	Total	Free	Total	Free
	(mg/g liver)		(Titer-1)		(Titer-1)	
3–4	4.7 ± 0.8	2.1 ± 0.5	9.5 ± 2.5	3.8 ± 1.0	22 ± 6	17 ± 5.2
12–14	4.8 ± 1.0	4.1 ± 2.5	6.0 ± 1.4	7.0 ± 1.3	18.5 ± 4.5	32 ± 0.5[d]
24–25	2.4 ± 0.3[e]	2.1 ± 0.4	8.8 ± 2.1	13 ± 1.9[d]	14.6 ± 0.6[d]	32 ± 0.5[d]

[a] Values reflect the means ± SD of four animals.
[b] α- and β-tubulin measured by enzyme-linked immunosorbent assay using bovine brain tubulin as standard.
[c] MAPS concentrations expressed as mean reciprocal titers ($Titer^{-1}$).
[d] Denotes significant difference versus young values ($P < 0.05$).
[e] Denotes significant difference versus young and mature values ($P < 0.05$).

be estimated accurately due to differences in organelle diameter relative to section thickness and the random orientation of the cytoskeletal elements in the plane of section. Small changes in this index may impair function, but remain morphologically undetectable. A diminution of microtubule number and length may compromise the vectorial movement of endocytic vesicles. Caron *et al.* (5) reported that very low doses of colcemid, e.g., <0.5 m*M*, markedly inhibited the processing of endocytosed ligands in cultured rat hepatocytes (5). These data suggest that the vesicle translocating function of microtubules is extremely sensitive to tubulin polymer levels.

The marked loss of polymerized tubulin between 3 and 12 months of age (75%), followed by an additional 12% decline between 12 and 24 months, correlates reasonably well with concomitant reductions of 85% and 3% in the hepatobiliary transport of IgA in mature and old rats, respectively (9). The large decline in mature rats seems to be due primarily to an increase in free or unpolymerized tubulin, whereas the later reduction in total tubulin content has only a minimal impact on polymerized tubulin. Clearly, aging appears to affect hepatic microtubules by two separate and sequential events, namely an increase in the free to total tubulin ratio and a decline in the total tubulin content, both of which contribute, albeit differentially, to a diminution of polymerized tubulin levels. The effect of aging on the free to total MAPS ratio is universal, i.e., a gradual, yet substantial, increase in MAP_1 and heat-stable MAPS (MAP_2 and tau). This shift to the free state may reflect a decrease in the affinity of MAPS for tubulin polymer and/or the concentration of polymerized tubulin. Factors that may contribute to reduced MAPS-tubulin binding include, but are not limited to, reduced dephosphorylation of MAPS or posttranslational modifications to polymerized tubulin (17). Age-related alterations in the capacity to phosphorylate or dephosphorylate a gene product are not without precedent (18). Furthermore, since MAPS directly affect monomer-polymer equilibrium by promoting tubulin assembly *in vitro* (14) and possibly *in vivo* (19), the loss of MAPS-tubulin affinity may also reduce the relative amount of tubulin assembled in old animals. Since we have shown that the *in situ* concentration of hepatocyte smooth-surfaced endoplasmic reticulum and the yield of hepatic microsomes decline substantially during aging in rats, we do not suspect that the age-related changes in polymerized tubulin and MAPS reflect concomitant differences in the binding of these moieties to membranes during isolation (20, 21). Since liver cells from old rats contain less membrane than those from young animals, we suggest that less, not more, tubulin or MAPS would be lost to recovery with increasing age. Our data lend credence to the supposition extended by Rao and Cohen (8) that aging may be accompanied by perturbations of microtubule function(s) which, in turn, contribute to the expression of biomarkers characteristic of normal aging (8). Subsequent studies will focus on the effects of aging on the synthesis and turnover of tubulin, as well as on its capacity to polymerize.

This study was supported in part by the Department of Veterans Affairs, NIH Grants AG07226, DK38436, and DK25878. The authors thank Rose K. Wang and Tuan Ma for their technical assistance.

1. Jones AL, Burwen AJ. Hepatic receptors and their ligands: Problems of intracellular sorting and vectorial movement. Semin Liver Dis **5**:136–146, 1980.
2. Maurice M, Feldmann G, Bellon B, Druet P. Increase in polymerized liver tubulin during stimulation of hepatic plasma protein secretion in the rat. Biochem Biophys Res Commun **97**:355–363, 1980.
3. Kacich RL, Renston RH, Jones AL. Effects of cytoshalasin D and colchicine on the uptake, translocation and biliary secretion of horseradish peroxidase and [14C] sodium taurocholate in the rat. Gastroenterology **85**:385–394, 1983.
4. Goldman IS, Jones AL, Hradek GT, Huling S. Hepatocyte handling of immunoglobulin A in the rat: The role of microtubules. Gastroenterology **85**:130–140, 1983.
5. Caron JM, Jones AL, Kirschner MC. Autoregulation of tubulin synthesis in hepatocytes and fibroblasts. J Cell Biol **101**:1763–1772, 1985.
6. Reaven EP. Quantitative analysis of tubulin and microtubule compartments in isolated rat hepatocytes. J Cell Biol **75**:731–742, 1977.
7. Horbach GJM, Cornelius MA, van Bezooijen CFA, Knook DL. Age-related changes in the synthesis of individual liver-specific proteins. Rev Biol Res Aging **3**:485–494, 1987.
8. Rao KMK, Cohen HJ. The role of the cytoskeleton in aging. Exp Gerontol **25**:7–22, 1990.
9. Schmucker DL, Gilbert R, Jones AL, Hradek GT, Bazin H. Effect of aging on the hepatobiliary transport of dimeric immunoglobulin A in the male Fischer rat. Gastroenterology **88**:436–443, 1985.
10. Schmucker DL, Daniels CK, Wang RK, Smith K. Mucosal immune response to cholera toxin in aging rats. I: Antibody and antibody-containing cell response. Immunology **6**:691–695, 1988.
11. Daniels CK, Schmucker DL, Jones AL. Age-dependent loss of dIgA receptors in the liver of Fischer 344 rats. J Immunol **134**:3855–3858, 1985.
12. Schmucker DL, Mooney JS, Jones AL. Stereological analysis of hepatic fine structure in the Fischer 344 rat. Influence of sublobular location and animal age. J Cell Biol **78**:319–337, 1978.
13. Patzelt C, Singh A, Le Marchand Y, Orci L, Jeanrenaud B. Colchicine-binding protein of the liver. Its characterization and relation to microtubules. J Cell Biol **66**:609–620, 1975.
14. Blose SH, Meltzer DI, Feramisco JR. 10-nm Filaments are induced to collapse in living cells microinjected with monoclonal and polyclonal antibodies against tubulin. J Cell Biol **98**:847–858, 1984.
15. Sloboda RD, Dentler WL, Rosenbaum JL. Microtubule-associated proteins and the stimulation of tubulin assembly in vitro. Biochemistry **15**:4497–4505, 1976.
16. Jones AL, Daniels CK, Burwen SJ, Schmucker DL. Age-related perturbations of vesicular transport and ligand processing in hepatocytes. In: Bianchi L, Holt PR, Butler RN, James OFW, Eds. Aging in Liver and Gastrointestinal Tract. Boston: MTP Press, pp181–190, 1988.
17. Murthy AS, Flavin M. Microtubule assembly using microtubule-associated protein MAP2 prepared in defined state of phosphor-

ylation with protein kinase and phosphatase. Eur J Biochem **137**:37–46, 1983.
18. Stein GH, Beeson M, Gordon L. Failure to phosphorylate the retinoblastoma gene product in senescent human fibroblasts. Science **249**:666–669, 1990.
19. Olmsted JB, Lyon HD. A microtubule-associated protein specific to differentiated neuroblastoma cells. J Biol Chem **256**:3507–3511, 1981.
20. Schmucker DL, Mooney JS, Jones AL. Age-related changes in the hepatic endoplasmic reticulum: A quantitative analysis. Science **197**:1005–1008, 1977.
21. Schmucker DL, Wang RK. Age-dependent alterations in rat liver microsomal NADPH cytochrome c (P-450) reductase during aging: A qualitative and quantitative analysis. Mech Aging Develop **21**:137–156, 1983.